Discordance of Disc-Fovea Raphe Angles Determined by Optical Coherence Tomography and MP-3 Microperimetry in Eyes With a Glaucomatous Hemifield Defect

Sotaro Mori, Takuji Kurimoto, Akiyasu Kanamori, Mari Sakamoto, Kaori Ueda, Yuko Yamada-Nakanishi, and Makoto Nakamura

Department of Surgery, Division of Ophthalmology, Kobe University Graduate School of Medicine, Kobe, Japan

Correspondence: Makoto Nakamura, Department of Surgery, Division of Ophthalmology Kobe University Graduate School of Medicine, 7-5-2, Kusunoki-cho, Chuo-ku, Kobe 650-0017, Japan; manakamu@med.kobe-u.ac.jp.

Submitted: December 4, 2018
Accepted: March 11, 2019

Citation: Mori S, Kurimoto T, Kanamori A, et al. Discordance of disc-fovea raphe angles determined by optical coherence tomography and MP-3 microperimetry in eyes with a glaucomatous hemifield defect. *Invest Ophthalmol Vis Sci*. 2019;60:1403–1411. https://doi.org/10.1167/iovs.18-26354

Purpose. The purpose of this study was to evaluate the concordance of a temporal raphe architecture estimated using optical coherence tomography (OCT) and MP-3 microperimetry.

Methods. We enrolled 25 eyes with either an upper or lower glaucomatous hemifield defect, as detected on the Humphrey visual field 30-2 test. A structural temporal raphe was extrapolated from visible end points of retinal nerve fiber bundles present in a perimetrically normal hemiretina on an en face Spectralis OCT image. A functional temporal raphe was drawn as a line from the fovea to the border of at least a 10-dB difference in sensitivity, at vertically adjacent test points, with at least three consecutive pairs among 25 test points placed at 8° to 18° from the fovea (2° intervals) on the MP-3. An angle determined by the optic disc center, the fovea, and the temporal raphe line (the DFR angle) was calculated. Correlations and agreement of the OCT- and MP-3–derived DFR angles and factors affecting discordance of the two estimates were evaluated.

Results. Despite no significant demographic differences, the functional DFR angle (mean ± SD, 171.8° ± 3.5°) was significantly larger than that of the structural DFR angle (166.5° ± 3.2°) in 14 eyes with upper hemifield defects and vice versa in 11 eyes with lower hemifield defects (163.4° ± 3.0° vs. 170.5° ± 3.2°). The mean deviation was significantly associated with the functional and structural DFR angle difference in eyes with only upper hemifield defects.

Conclusions. The structural temporal raphe was more deviated to the perimetrically normal hemiretina side than to the functional temporal raphe, thereby suggesting that a structural change may precede a functional loss.

Keywords: glaucomatous hemifield defect, MP-3 microperimeter, nasal step, optical coherence tomography, temporal raphe

A nasal step is a visual field defect that is seen in the nasal visual field and obeys the horizontal meridian. It is confined to an area in either the upper or lower hemifield and is a characteristic pattern of early visual field loss in an eye with glaucomatous optic neuropathy.[1] This unique pattern of visual field defect may result from retinal nerve fibers that were separated, either superiorly or inferiorly, by a horizontal meridian, termed the temporal raphe (TR).[1] Based on Vrabec's study of enucleated human eyes,[2] the TR consists of three parts: the perpendicular fascicles, the oblique fascicles, and a triangular area, where the fascicular density is low. Until recently, the TR was considered a straight line connecting the fovea and the triangular area, which extends to the temporal periphery.

However, clinicians encounter patients with glaucoma who show a dominantly hemifield visual field defect but have a scotoma that is contiguous to the hemifield defect and exceeds the horizontal meridian. Recent advances in imaging technology, such as adaptive optics scanning laser ophthalmoscope (AO-SLO) and optical coherence tomography (OCT), can clearly visualize the nerve fiber bundles in vivo.[3–6] These studies demonstrated that the TR orientation is highly variable among individuals. Moreover, it is not always parallel to the horizontal meridian or a simple continuation of the line connecting the optic disc center and the fovea. Additionally, such variability in the TR orientation may cause structure–function dissociation at the TR region. A previous study predicted that, in 12% of patients with glaucoma, a scotoma around the nasal step region would map to the opposite hemiretina, and consequently, the opposite pole of the optic disc from the canonically expected position.[7]

Furthermore, recent studies also demonstrated that the reflectance of an optic nerve fiber bundle in a perimetrically normal hemiretina was already retarded in glaucomatous eyes with a hemifield defect.[4,6] Furthermore, the TR gap was wider in eyes with glaucoma than in controls,[4,6] suggesting the structural change may precede the functional loss in the apparently normal-looking hemiretina of eyes with a hemifield defect. Previous studies used the Humphrey visual field (HVF) test as a functional evaluation[4,5,7–9]; therefore, the precise structure–function correlation at the TR region has not been elucidated. The HVF test has several disadvantages as it relates to assessing the structure–function relationship at the TR region. On the HVF test, the TR region test points are sparsely

located and indirectly stimulated. They are tested by a stimulus light that is projected onto a dome-shaped screen.

The novel MP-3 microperimeter (NIDEK Co., Ltd., Aichi, Japan) measures visual field sensitivity by projecting a target light directly onto the region of interest on the retina rather than onto a screen.[10,11] The retina position is automatically tracked and the stimulus location is aligned accordingly, resulting in precise determination of retinal test locations stimulated at each target presentation. Compared with the HVF test, this full-autotracking system makes it possible to measure sensitivities more accurately, at exact test points. The MP-3 has a wider dynamic range than the older version, MP-1; thus, visual sensitivities between 0 and 34 dB can be measured on its background luminance of 31.5 apostilb (asb), which is identical to the HVF test. Clinical application of the MP-3 is increasing as it relates to evaluating glaucoma[12] and other eye diseases, such as retinitis pigmentosa.[13,14]

Another issue that should be considered when assessing structure–function correlation is the parameter to be evaluated. Previously, either a disc-fovea (DF) angle or a TR angle, or both, were evaluated.[15–17] These angles were referenced with a horizontal line on the fundus photograph or imaging captured by other devices such as an OCT. However, it is impractical to set a true horizontal line on such a photograph and imaging, given eye rotation and head posture variability among and within individuals.[8,9] For this reason, recent studies have used an obtuse angle that is determined by three landmarks: the optic disc, the fovea, and the TR. This angle is herein termed the DFR angle, which is not influenced by eye rotation/head posture.[3,8,9,17]

The purpose of this study was to evaluate the structure–function correlation at the TR region using an OCT and the MP-3 in glaucomatous eyes with a hemifield defect. More specifically, we measured the DFR angles using these two modalities in the same patients. The OCT- and MP-3–derived DFR angles were subsequently compared. Additionally, the concordance or discordance of the two values was evaluated. If values were discordant, factors affecting the structure–function dissociation were also evaluated.

Materials and Methods

Subjects

This is a prospective case series. The study protocol was approved by the ethical committee of Kobe University Hospital and registered on the university hospital's Medical Information Network-Clinical Trial Registry (UMIN0000026200). The study was conducted in accordance with the tenets of the Declaration of Helsinki.

Informed consent was orally obtained from each participant and stored in the hospital database in accordance with the regulations of the Japanese Government's Guidelines for Epidemiologic Study (2008). These guidelines do not require acquisition of written consent for a clinical study that does not conduct an invasive procedure if the protocol were posted at the outpatient clinic to notify study participants.

Subjects had primary open angle glaucoma and regularly visited the glaucoma outpatient clinic of the Kobe University Hospital between March 2017 and September 2018. These subjects showed reproducible visual field defects that were confined to either the upper or lower hemifield as detected on the HVF analyzer, using the Swedish Interactive Thresholding Algorithm (SITA) 30-2 program (Carl Zeiss Meditec, Dublin, CA, USA) (Fig. 1A), as previously reported.[18] The subjects also agreed to undergo both a TR imaging by Spectralis OCT (Heidelberg Engineering, Heidelberg, Germany) and a visual field testing by MP-3 (NIDEK Co., Ltd.) within 3 months of the last HVF testing. Subjects had to be between 20 and 80 years old, have at least three contiguous points with $P < 0.05$, one of which showed $P < 0.01$ on a pattern deviation plot and a mean deviation (MD) between −2 and −15 dB, and best-corrected Landolt decimal visual acuity equivalent to 20/20 or better. Patients with ocular or systemic diseases (other than glaucoma and uncomplicated pseudophakia) that affect the retina and optic nerve have a spherical equivalent refractive error more myopic than −8 diopters (D), with unreliable HVF test results, showing either the fixation loss ≥20%, or the false-positive or false-negative error rates ≥25%, and abnormal HVF test points that went over the horizontal meridian were all excluded. In patients with both eyes that met the above criteria, the right eyes were selected for analyses, and left eye data were converted to the right eye format. Consequently, 25 eyes in 25 patients met the above criteria.

All subjects underwent comprehensive ophthalmic evaluations, including refraction, best-corrected Landolt decimal visual acuity, slit-lamp biomicroscopy, gonioscopy, Goldmann applanation tonometry, axial length, dilated funduscopy, fundus photography, and Spectralis OCT and MP-3 measurements. The axial length was measured using IOL Master 500 (Carl Zeiss Meditec).[19] Spectralis OCT and MP-3 measurements were conducted on the same day.

Structural DFR Angle Measurement

Structurally, the DFR angle measurement was based on a composite image of a fundus photograph and a Spectralis OCT image (Figs. 1B, 1E) after the pupil was dilated. In brief, retinal nerve fiber images were generated from 10° × 30° high density volume scans consisting of 391 B scans (11-μm separation). Each B scan was averaged from nine individual images. A transverse section analysis (version 6.0.) was used to visualize en face reflectance images of the retinal nerve fiber bundle trajectories, which were determined by retinal layer segmentation and by setting the nerve fiber layer as a reference plane, essentially according to the method reported by Chauhan et al.[5] The OCT image was overlaid on the fundus photograph based on major vessels and the fovea orientation.

The center of the optic disc was determined according to a study by Jonas et al.[20] In brief, the center of the disc was determined as the middle point of the line connecting the middle points of the minimal and maximal disc diameters. The location of the fovea was assessed as the location of the foveal reflex in eyes with foveal reflex, as the center of the macula wall reflex in eyes that showed a macular wall reflex but no foveal reflex, and as the center of the apparently avascular zone in eyes that did not demonstrate any macular reflexes. A DF line was drawn on the composite image by connecting the optic disc center and the fovea. This determined a DF angle against the arbitrary horizontal line ("a" in Figs. 1B, 1D).

Subsequently, the endpoints of the nerve fiber bundles that came from perimetrically normal hemiretina were manually plotted, from the perifovea to the temporal periphery, the number of which was determined depending on the visibility. It ranged from 25 to 40 with approximately 250 μm interval, starting from an endpoint closest to the temporal extreme of the fovea. A TR line was calculated and drawn by the least square method using Image J software (National Institute of Health, Bethesda, MA, USA). A TR angle was defined as an acute angle, determined by the arbitrary horizontal line, and the TR line ("b" in Figs. 1B, 1D). Following this, the structural (or OCT-derived) DFR angle was

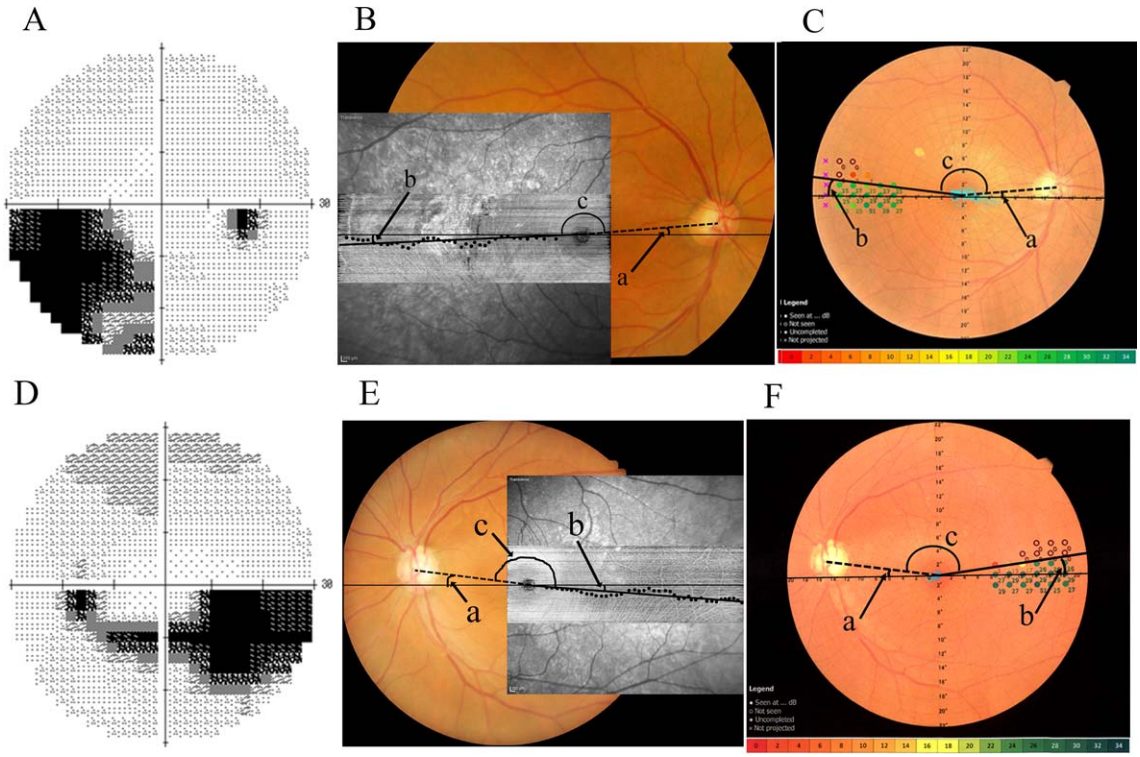

FIGURE 1. Examples of how to determine structural and functional DFR angles. (**A**–**C**) Example of a right eye of one identical patient. (**D**–**F**) Example of a left eye of another identical patient. (**A**, **D**) Grayscales of the HVF test. (**B**, **E**) Composite images of OCT images superimposed on fundus photographs. (**C**, **F**) MP-3 microperimetric results. Angle "a," a DF angle that was determined by a *straight line* that is horizontally crossing and evenly dividing the images vertically and a *dashed line* connecting the center of the optic disc and the fovea, termed a DF line. Angle "b," a temporal raphe angle that was determined by the *horizontal line* and an oblique *straight line* that was extrapolated from a *dotted curve*, end points of the retinal nerve fiber bundles coming from the perimetrically normal inferior hemiretina (**B**, **D**), or that was a border of at least 10-dB difference in sensitivity at vertically adjacent test points with at least three consecutive pairs (**C**, **E**), termed a TR line. Angle "c" is the DFR angle that is determined by the DF line and the TR line. The OCT image is acquired by the transverse section analysis mode of Spectralis OCT. Note that the inferior visual field defects detected on the HVF test grayscales obey the horizontal lines, whereas the TR lines are not parallel to the horizontal lines, and the DFR angles are <180° when determined by both OCT and MP-3.

calculated as an obtuse angle determined by the DF line and the TR line ("c" in Figs. 1B, 1D).

Functional DFR Angle Measurement

Functionally, the DFR angle was calculated based on MP-3 data (Figs. 1C, 1F). As with the classical HVF test, the MP-3 measurement was conducted using a 4-2 full-threshold staircase strategy with the standard Goldmann III stimulus size. The maximum luminance of the MP-3 is 10,000 asb, and the stimulus dynamic range is between 0 and 34 dB.[10–14] Only reliable test results (a false-positive rate of <20% and a false-negative rate of <25%) were used in the analyses, as in the HFV SITA test results set in the present study. A fixation loss is not applicable because the MP-3 has an autotracking system, making it possible to project the stimulus only at predefined retinal positions. As shown in Figures 1C and 1F in the present study, visual field sensitivity at the TR region was measured by stimulating 25 test points that were aligned in a wedge shape and placed between 8° and 18° apart from the fovea to the temporal periphery with a 2° interval. The visual field sensitivities were expressed as closed circles in cold colors (green or blue) when the sensitivities were better than 24 dB, whereas warmer colors (yellow, orange, or red) and open circles were used to express sensitivities worse than 18 and 0 dB, respectively. The built-in software automatically aligned and expressed the coordinate axes on the fundus photograph, which was simultaneously acquired with the sensitivity measurement at the designated test points, where the fovea was located (0, 0). A line from the fovea to the border with at least a 10-dB difference in sensitivity at vertically adjacent test points with at least three consecutive pairs was extrapolated and drawn by the least square method using Image J software (National Institutes of Health). This line was considered a nasal step border or a functional TR line. An angle determined by this line and an arbitrary horizontal line ("b" in Figs. 1C, 1F) was defined as a functional TR angle. The functional (or MP-3–derived) DFR angle was then calculated as an obtuse angle, determined by the DF line and the functional TR line ("c" in Figs. 1C, 1F).

Statistical Analysis

Statistical analyses were performed using MedCalc (version 18.2.1; MedCalc Software, Mariakerte, Belgium) with a type I error for significance set at $P < 0.05$.

To validate the agreement of measurement by two examiners (SM and TK), intraclass correlation coefficients (ICCs) were obtained for the OCT-derived and MP-3–derived DFR angles. Comparisons between DFR angles that were determined by OCT and MP-3, within the same hemifield defect group, were made using the paired *t*-test. Correlations between the MP-3–derived and the OCT-derived DFR angles were tested using Pearson's correlation coefficients. The associations of the differences in the MP-3– and OCT-derived DFR angles with age, axial length, refractive error, and MD were tested using Spearman rank correlation coefficients.

Table. Subject Characteristics

Parameter	Upper Defect	Lower Defect	*P* Value
Number	14	11	
Sex (number of men)	7	5	1.00*
Laterality (number of right eyes)	9	3	0.11*
Age (y)	64.1 (13.9)	58.4 (12.7)	0.19†
Mean deviation (dB)	−8.14 (3.99)	−7.50 (3.59)	0.58†
Axial length (mm)	24.42 (1.39)	24.49 (1.77)	0.66†
Spherical equivalent (D)	−2.3 (3.3)	−2.8 (2.8)	0.70†
DFR angle (MP-3) (degree)	171.8 (3.5)	163.4 (3.0)	0.002†
DFR angle (OCT) (degree)	166.5 (3.2)	170.5 (3.2)	0.004†

* Fisher's exact test.
† Mann–Whitney *U* test.

Bland–Altman plot analyses were made to evaluate whether a systematic bias of differences between the MP-3– and OCT-derived DFR angles was present.

Results

The Table summarizes the patients' demographic characteristics. Fourteen eyes of 14 patients had upper hemifield defects, whereas 11 eyes of 11 patients had lower hemifield defects. No significant differences in the proportion of sex and eye laterality, age, MD, axial length, and spherical equivalent refractive error were noted between those with the upper and lower hemifield defects. However, the DFR angle was significantly different between the two groups. When measured using MP-3, the upper defect group had a significantly wider DFR angle (171.8°) than the lower defect group (163.4°). In contrast, the upper defect group, when measured using OCT, had a significantly narrower DFR angle (166.5°) than the lower defect group (170.5°). The ICC for the MP-3-derived DFR angle determined by two examiners was 0.937 (95% confidence interval, 0.858–0.972) and that for the OCT-derived one was 0.972 (95% confidence interval, 0.936–0.988), indicating excellent agreement. Hence, for the sake of clarity, only data measured by TK are shown herein.

Figure 2 illustrates histograms of the DFR angle distribution. The difference in the DFR angle, measured using MP-3 and OCT, was statistically significant in both the upper visual hemifield defect (paired *t*-test; $P = 0.0001$) and in the lower visual hemifield defect ($P < 0.0001$). Therefore, the MP-3–derived, functionally determined DFR angle was wider than the OCT-derived, structurally determined DFR angle in eyes with upper hemifield defects, whereas it was the opposite in eyes with lower hemifield defects.

Figure 3 depicts scatter plots of the DFR angles measured using MP-3 versus those measured using OCT. There was a significant correlation between the two measurements in eyes with lower hemifield defects ($r = 0.774$, $P = 0.0051$), but there was no significant correlation in those with upper hemifield defects ($r = 0.398$, $P = 0.159$).

Figure 4 shows the Bland–Altman plot of the difference between the OCT-derived and the MP-3–derived DFR angles against the mean of these two measurements. Although there was no proportional bias, there was a fixed bias between the DFR angle estimates measured using the two modalities. In other words, in eyes with upper hemifield defects, the MP-3 measurements were consistently larger than the OCT measurements, with a mean difference of 5.5°. In eyes with lower

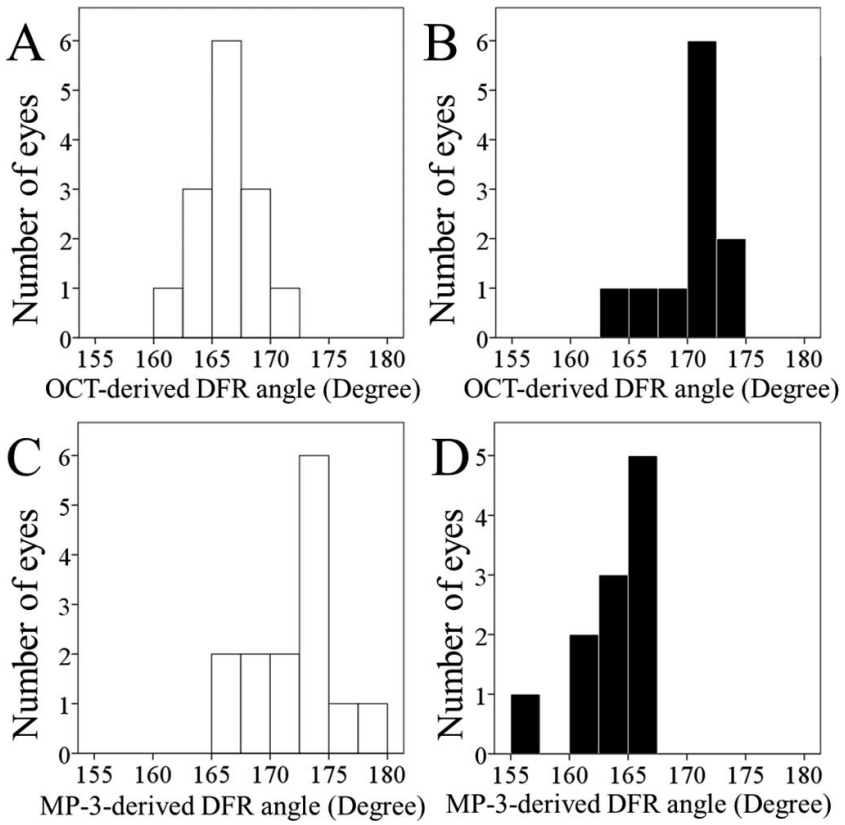

Figure 2. Histograms of DFR angles. (**A**, **B**) DFR angle distributions when measured using an OCT. (**C**, **D**) DFR angle distributions when measured using an MP-3 microperimeter. (**A**, **C**) Eyes with an upper hemifield defect. (**B**, **D**) Eyes with a lower hemifield defect.

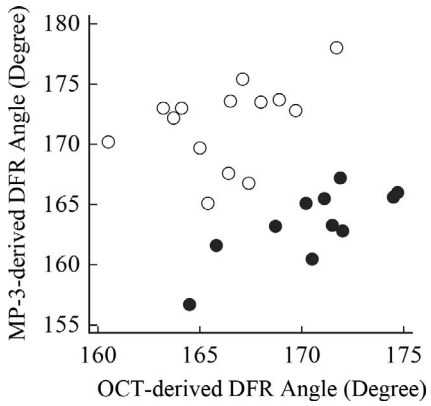

FIGURE 3. Scatter plots of DFR angles measured using an MP-3 microperimeter against those measured using OCT. *Open circles* indicate eyes with an upper hemifield defect, whereas *closed circles* indicate those with a lower hemifield defect. Significant correlations between two measurements in the lower hemifield defect patients were seen (Pearson correlation coefficient [r] = 0.774, P = 0.0051), whereas no significant correlations in the upper hemifield defect patients were observed (r = 0.398, P = 0.159).

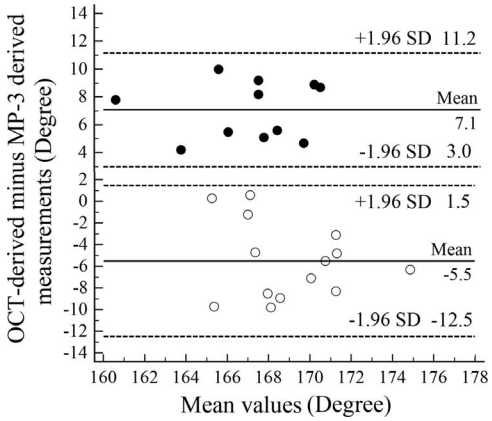

FIGURE 4. Bland-Altman plots to evaluate the presence or absence of a systematic bias in terms of the correlation of the difference in the DFR angle measured using OCT and an MP-3 microperimeter with the average of the two. Regression analyses were separately conducted in eyes with an upper hemifield defect (*open circles*) and a lower hemifield defect (*closed circles*). SD, standard deviation.

hemifield defects, the OCT measurements were consistently larger than the MP-3 measurements with a mean difference of 7.1°. This was irrespective of the extent of the average of the two measurements. On the other hand, when the two groups were combined, the difference between the two values was approximately zero.

Figure 5 illustrates the correlations of the differences in the DFR angles measured using the two modalities with age, axial length, spherical equivalent refractive error, and MD. As shown in Figures 5A–C, there was no significant association of the difference in the OCT-derived and MP-3–derived DFR angles with age, axial length, or refractive error in eyes with either upper or lower hemifield defects. On the other hand, as shown in Figure 5D, there was a significant correlation between the DFR angle difference, measured using the two modalities, and the MD in eyes with upper hemifield defects (r = 0.749, P = 0.002), indicating that the more advanced the visual field defect, the greater the DFR difference. In comparison, there was a similar trend, although insignificant, in eyes with lower hemifield defects (r = –0.555, P = 0.0767).

Figure 6 shows two representative cases, one of which had very close DFR angles measured using MP-3 (165.4°) and OCT (165.1°) (Figs. 6A, 6B), whereas the other had a substantial difference between the MP-3–derived DFR angle (173.0°) and the OCT-derived DFR angle (164.1°) (Figs. 6C, 6D). Note that the latter exhibited a worse visual field defect (MD = –10.94 dB) than the former (MD = –5.45 dB).

Figure 7 shows schematic diagrams of DFR angles determined by Spectralis (black arcs) and MP-3 (red arcs) in eyes with upper hemifield defects (Fig. 7A) and with lower hemifield defects (Fig. 7B). TR lines determined by Spectralis are expressed using black solid lines (a), whereas those determined by MP-3 are expressed using red dotted lines (b). These TR lines, both OCT-derived and MP-3–derived, are shown as a retina view. Note that the structural TR lines are deviated toward a perimetrically normal hemiretinal side (i.e., the perimetrical TR lines toward a structurally damaged hemiretinal side).

DISCUSSION

The present study found that an angle (the DFR angle) determined by three landmarks (the optic disc center, the fovea, and the TR), using MP-3 and Spectralis OCT, was differently distributed between eyes with upper hemifield defects and those with lower hemifield defects (Figs. 2–4, 6, and 7). In other words, those with upper hemifield defects showed significantly wider DFR angles than those with lower hemifield defects when the DFR angle was determined using MP-3, whereas the opposite applied when it was determined using OCT.

Several studies previously calculated the DFR angle in healthy volunteers using imaging technologies. Huang et al.[3] measured the DFR angle using AO-SLO and estimated it to be 170.3° ± 3.6° in 11 young subjects. Bedggood et al.[17] measured it using spectral domain OCT and reported it to be 172.4° ± 2.3° in 15 young volunteers. Furthermore, a recent study by Bedggood et al.,[8] in which the TR orientation was automatically estimated by the vertically oriented nerve fiber intensity, measured using the OCT macular cube, reported that the DFR angle was 173.5° ± 3.2° in control eyes and 174.2° ± 3.4° in eyes with primary open angle glaucoma. The study also reported that the two values were not statistically different. Although direct comparisons of data between the present and previous studies may be challenging because of different demographic backgrounds and the methodology of DFR angle calculation, the present estimates of the DFR angle agree with previous values, overall.

In the present study, however, the average DFR angle in those with upper hemifield defects was 171.8° and 166.5°, when measured using MP-3 and OCT, respectively, whereas that in those with lower hemifield defects was 163.4° and 170.5°, respectively. Therefore, the DFR angle obtained was dependent on the modality of measurement and the side of the glaucomatous hemifield change. Such a difference between the OCT-derived (structurally determined) DFR angle and the MP-3–derived (functionally determined) DFR angle was thought to be strictly due to the TR location estimated by the two modalities, given that the optic disc-fovea angle was set as identical within the same eyes when the two modalities were used in the present study. The difference in the OCT-derived and MP-3–derived DFR angles was also not due to the variation of the arbitrary horizontal midline set on the fundus photograph because the horizontal line was not used for the calculation of the DFR angles in this study. Therefore, the difference in the DFR angles, as defined by the two modalities, was not an artifact influenced by eye rotation or head posture

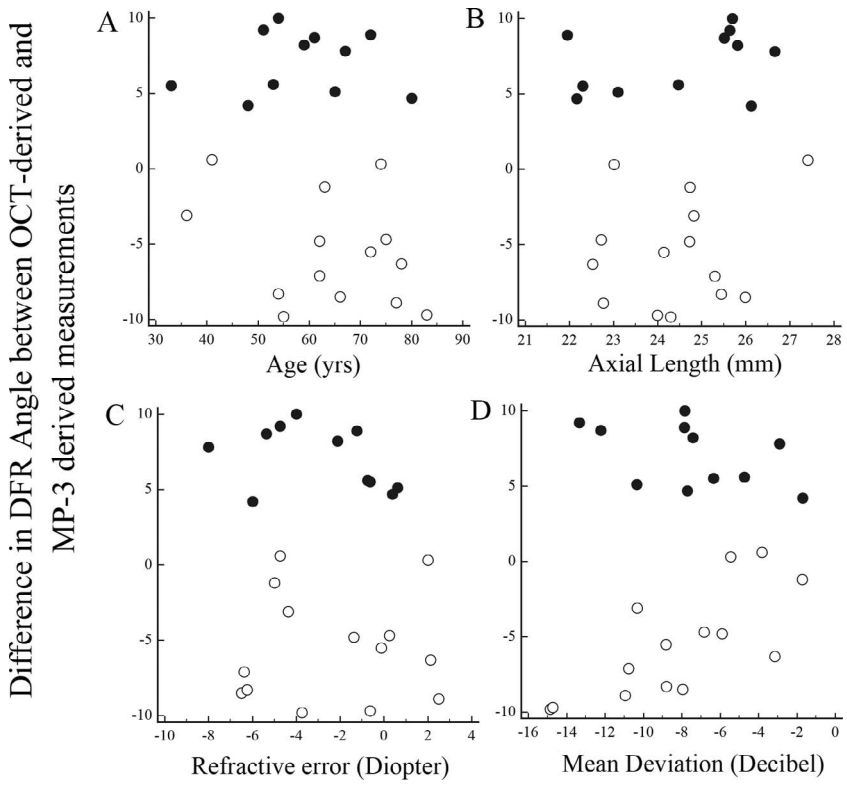

Figure 5. Scatter plots of differences in DFR angles measured using OCT and an MP-3 microperimeter against age (**A**), axial length (**B**), spherical equivalent refractive error (**C**), and MD of the HVF test (**D**). *Open circles* indicate patients with upper hemifield defects, whereas *closed circles* those with lower hemifield defects. There were no significant correlations between the DFR angle differences and either age, axial length, or refractive error. There was a significant correlation between the DFR difference measured using the two modalities and MD in the eyes with an upper hemifield defect (Spearman's rank correlation coefficient [ρ] = 0.749; $P = 0.002$), whereas such a significant correlation was not found in the eyes with a lower hemifield defect (ρ = –0.555, $P = 0.077$).

variability.[3,8,9,17] Although such a difference in the OCT-derived DFR angles between eyes with upper and lower hemifield defects was not described in the study by Bedggood et al.,[8] their study included patients with glaucoma with various types of visual field defects that were not classified as either upper or lower hemifield defects. Therefore, the differences in DFR angles in patients with glaucoma with upper and lower hemifield defects may have been canceled in the study by Bedggood et al.[8] In fact, Figure 4 shows that, when the two groups were combined, the difference in the DFR angle measurements using the two modalities was close to zero.

The present study determined the TR, when OCT was used, by extrapolating the end points of nerve fiber bundles present in the hemiretina of normal visual fields on both HVF and MP-3. Previously, Huang et al.[4] reported that there was a gap at the TR region between end points of vertically oriented retinal nerve fiber bundles from the upper and lower hemiretinas. In addition, such a gap was wider in glaucomatous eyes, even with milder visual field damage of less than −3.5 dB at the TR region, than in control eyes.[4] This may have been, at least in part, because the reflectivity of the retinal nerve fiber bundle may already be retarded in the perimetrically normal hemiretina. Ashimatey et al.[6] stated that it was common to find locations of substantial reflectance abnormality, with mild to no perimetric abnormality at the TR region, probably due to disruption of the microtubule cytoarchitecture or nerve fiber bundle density.[21–24] They speculated that an abnormality in the raphe can be quantified using changes in the reflectance or width of the nerve fiber bundles in addition to an increase in the raphe gap.[6] In eyes with either hemifield defect in the present study, the TR line, as defined by OCT, was estimated to be deviated toward the perimetrically undamaged hemiretina side compared with that as defined by MP-3. Such a trend may be supported by either of the above theories (i.e., the TR gap widening or the reduced nerve fiber bundle reflectance in the perimetrically normal hemiretina in glaucomatous eyes), indicating that the structural change may precede the functional change at the TR region. A number of previous studies reported that the hemiretinal side even with a normal visual field exhibited structural changes detected as thinning of the circumpapillary retinal nerve fiber layer and the inner retinal layer thickness.[25–27] The present findings may support these previous reports.

However, the above theories alone may not be able to account for the MP-3–derived DFR angle in those with lower hemifield defects being as narrow as 163.4°. As mentioned earlier, previous studies demonstrated the DFR angle in controls to be approximately 170°.[3,8,17] The present study has also disclosed that those with upper hemifield defects showed an MP-3–derived DFR angle of 171.8° and those with lower hemifield defects exhibited the OCT-derived DFR angle of 170.5°. These are close to previously obtained values. Therefore, the OCT-derived DFR angle became narrower than the MP-3–derived, functionally determined DFR angle, in eyes with upper hemifield defects (lower hemiretinal damage). This is because the TR gap was widened as a result of the reduced OCT reflectivity of the nerve fiber bundles in the upper hemiretina. However, if such a phenomenon also happened a posteriori in eyes with inferior hemifield defects (the upper hemiretinal damage), and the TR gap had widened because of the reduced reflectivity of the nerve fiber bundles present in the perimetrically normal lower hemiretina, the OCT-derived

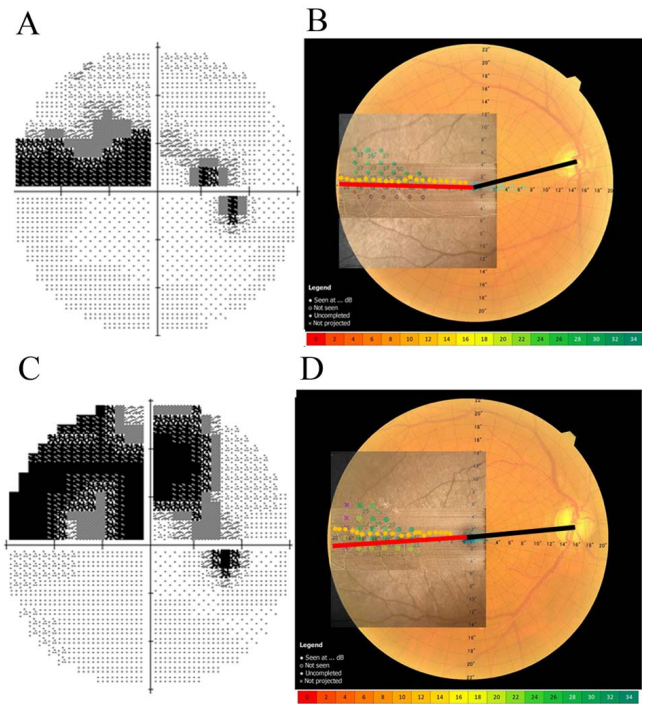

FIGURE 6. Examples of eyes that showed structural and functional concordance (**A**, **B**) and discordance (**C**, **D**), respectively, in terms of measurement of a DFR angle. (**A**, **C**) Grayscale of the HVF test. (**B**, **D**) Composite images of Spectralis OCT and MP-3 microperimeter. *Yellow dotted lines* indicate end points of the retinal nerve fiber bundles coming from the perimetrically normal upper hemiretina detected on the Spectralis OCT. *Red lines* indicate borders of at least a 10-dB difference in sensitivity at vertically adjacent test points with at least three consecutive pairs detected on the MP-3. *Black lines* indicate lines connecting the center of the optic disc and the fovea. Note that the concordant eye has less visual field damage detected on the HVF test than the discordant eye.

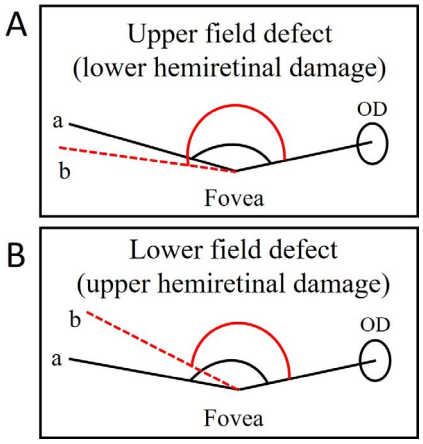

FIGURE 7. Schematic diagrams of structurally and functionally determined DFR angles in eyes with upper and lower glaucomatous hemifield defects. (**A**) An eye with the upper hemifield defect. (**B**) An eye with the lower hemifield defect. A *black line* designated as "a" indicates a temporal raphe determined by Spectralis OCT. A *red dotted line* designated as "b" indicates a temporal raphe determined by MP-3. Both temporal raphe lines are shown as a retina view. *Black curves* indicate the OCT-derived DFR angle, whereas *red curves* do the MP-3–derived DFR angle. OD, optic disc.

DFR angle in those eyes should have been enlarged to around ≥175°, rather than 170.5°, which is almost the same as the reported control. Also, the MP-3–derived DFR angle should have been measured to be around 170° instead of 163.4°, which was a much narrower angle than expected. Therefore, a complementary or alternative explanation is needed to account for the combinations of structurally and functionally determined DFR angles that were found in eyes with lower hemifield defects.

Assuming a wider raphe gap was responsible for the structure–function dissociation at the TR and that the functionally determined DFR angle was not yet changed from the naïve condition, it may be reasonable to think that eyes with lower hemifield defects had narrower DFR angles than controls a priori. The nerve fiber bundles in the upper hemiretina in an eye with such a congenitally extraordinary narrow DFR angle may be vulnerable to mechanical or some other stress, resulting in the lower hemifield defect. This hypothesis may be supported by the present findings that a correlation between the disease severity and the difference in the OCT- and MP-3–derived DFR angles was definitely present in those with upper hemifield defects but was not very clear in those with lower hemifield defects. The more advanced the visual field defect, the wider the difference in eyes with upper hemifield defects. This can be accounted for by the theory that the raphe gap widened in an acquired fashion in accordance with disease progression. In contrast, such an association was weak and not statistically significant between the DFR angle differences measured using the two modalities and the MD in eyes with lower hemifield defects. In other words, irrespective of disease severity, eyes with inferior hemifield defects had a consistent DFR angle difference of around 7.1° between the two modalities used. This may indicate that eyes with inferior hemifield defects innately have a narrow DFR angle to some degree. Regarding the fact that the DFR angle is <180°, Tanabe et al.[9] also speculated that perhaps there are some interactions between the position of the optic disc and the retinal nerve fiber layer trajectories during development that bears an obtuse DFR angle.

The present study found no significant correlation in the DFR angle difference measured using the two modalities with age, axial length, or refractive error. The previous study by Huang et al.[4] showed that the raphe gap widened with advancing age in healthy eyes, whereas the study by Bedggood et al.[8] did not show such an association. One possible explanation for these inconsistent results is that age-dependent changes in the nerve fiber bundle reflectance may be less than the changes induced by glaucoma. According to Bedggood et al.,[8] there was no significant association of the DFR angle with axial length.

Among retinal ganglion cells (RGCs) that reside in the TR region, a minor population of RGCs projecting their axons to the horizontally opposite, healthy hemiretina is more likely to be preserved against glaucomatous damage than the majority of the population of RGCs that project their axons to the damaged hemiretina.[2,28] From this perspective, the observation that the "TR" defined by the MP-3 measurement tended to be shifted toward the damaged hemifield (hemiretina) may be accounted for, not only by the retarded reflectivity of retinal nerve fibers in the perimetrically normal hemiretina, but also by the relatively greater number of RGCs that are located in the damaged hemiretina but project their axons to the opposite, healthy hemiretina, and are preserved in comparison to RGCs located in the damaged hemiretina that also project their axons into the same damaged hemiretina. If this is the case, our findings do not necessarily indicate that the structural change in the perimetrically normal hemiretina precedes the functional damage. Instead, it may suggest that the balance of the ratio of interdigitated retinal nerve fibers in the TR region was

changed due to glaucomatous insults on the retinal nerve fibers and, subsequently, the RGCs.

On the other hand, this scenario does not seem to be able to explain the difference in the degree of correlation of the disease severity with the degree of structure–function dissociation between eyes with upper and lower hemifield defects. If the proportion of interdigitated retinal nerve fibers changes depending on the disease severity, the degree of structure–function dissociation should become larger in proportion to the disease progression in eyes with lower hemifield defects as it does in those with upper hemifield defects. Nevertheless, the difference was almost consistently around 7.1° in eyes with lower hemifield defects, irrespective of the disease severity. This finding suggests that factors other than the change in proportion of the interdigitated retinal nerve fibers are more likely to be involved in the structure–function dissociation, at least in eyes with lower hemifield defects.

There are receptive fields of the RGCs in the "normal" area of the retina that extend into the area without visible axon bundles. This raises the possibility that the presence of RGCs with a wider receptive field, of which dendrites cannot be visualized by OCT, may have affected the structural and functional DFR angle dissociation, at least in eyes with upper hemifield defects (i.e., the lower hemiretinal damage). In other words, the RGCs with a narrower receptive field may have been more selectively and earlier damaged than the RGCs with a wider receptive field in the "normal" upper hemiretina, given that the structure–function dissociation was significantly associated with disease severity (the worse MD) in these eyes. This ultimately means that at least a fraction of the population of RGCs (i.e., RGCs with a narrower receptive field) is decreased prior to manifestation of the visual field defect. This supports our original conclusion that the structural change may precede the functional loss in the perimetrically normal hemiretina at the TR region in glaucomatous eyes.

This study also has other limitations. Small sample size may be a reason that the correlation between the MP-3– and OCT-derived DFR angle difference and the MD, in those with lower hemifield defects, did not show statistical significance. If this is true, then the above hypothesis of an innately narrow DFR angle in eyes with lower hemifield defects may not be justified. Although the TR was assumed to be a straight line to compare the MP-3– and the OCT-derived DFR angles in the present study, this was not actually the case when measurements were conducted using the OCT. Finally, we set, in the MP-3 analysis, a functional border as at least a 10-dB difference in sensitivity, at vertically adjacent test points with at least three consecutive pairs. MP-3 does not have an age-corrected normative database, which practically makes it difficult to determine whether the subtle reduction of sensitivity at a particular stimulated point is pathological or not (i.e., aging effect or disease induced). This is why we set a relatively large sensitivity gap as a nasal step border. We chose "10 dB" as a specific threshold of the border according to a recent study by other investigator, who also focused on the nasal step in glaucomatous eyes.[12] Given that there is no established definition of the nasal step in terms of visual field sensitivity, we think it cannot be helped to set a functional horizontal border using arbitrary criteria to some degree. However, we cannot completely rule out the possibility that this 10-dB criteria may have affected the decision of the functional border. Therefore, a more complex structure–function correlation may exist at the TR region in glaucomatous eyes. Further accumulation of patients and refinement in the measurement of the TR are required.

In conclusion, the OCT-derived (structurally determined) TR was more deviated to the perimetrically normal hemiretina side than to the MP-3–derived (functionally determined) TR, in the disease severity-dependent fashion, particularly in eyes with upper hemifield defects. This was essentially responsible for the difference in the DFR angle as measured using the two modalities in eyes with glaucomatous hemifield defects. Such structure–function dissociation suggests that the structural change may be present even in the perimetrically normal hemiretina.

Acknowledgments

A part of this study was presented at the 23rd International Visual Field and Imaging Symposium held in Kanazawa, Japan, 2018.

The authors thank "Enago (www.enago.jp)" for the English language review.

Supported by Grant 18K09447 from the Japan Society for the Promotion of Science (MN).

Disclosure: **S. Mori**, None; **T. Kurimoto**, None; **A. Kanamori**, None; **M. Sakamoto**, None; **K. Ueda**, None; **Y. Yamada-Nakanishi**, None; **M. Nakamura**, None

References

1. Werner EB, Beraskow J. Peripheral nasal field defects in glaucoma. *Ophthalmology*. 1979;86:1875–1878.
2. Vrabec F. The temporal raphe of the human retina. *Am J Ophthalmol*. 1966;62:926–938.
3. Huang G, Gast TJ, Burns SA. In vivo adaptive optics imaging of the temporal raphe and its relationship to the optic disc and fovea in the human retina. *Invest Ophthalmol Vis Sci*. 2014; 55:5952–5961.
4. Huang G, Luo T, Gast TJ, Burns SA, Malinovsky VE, Swanson WH. Imaging glaucomatous damage across the temporal raphe. *Invest Ophthalmol Vis Sci*. 2015;56:3496–3504.
5. Chauhan BC, Sharpe GP, Hutchison DM. Imaging of the temporal raphe with optical coherence tomography. *Ophthalmology*. 2014;121:2287–2288.
6. Ashimatey BS, King BJ, Malinovsky VE, Swanson WH. Novel technique for quantifying retinal nerve fiber bundle abnormality in the temporal raphe. *Optom Vis Sci*. 2018;95:309–317.
7. McKendrick AM, Denniss J, Wang YX, Jonas JB, Turpin A. The proportion of individuals likely to benefit from customized optic nerve head structure-function mapping. *Ophthalmology*. 2017;124:554–561.
8. Bedggood P, Nguyen B, Lakkis G, Turpin A, McKendrick AM. Orientation of the temporal nerve fiber raphe in healthy and in glaucomatous eyes. *Invest Ophthalmol Vis Sci*. 2017;58: 4211–4217.
9. Tanabe F, Matsumoto C, McKendrick AM, Okuyama S, Hashimoto S, Shimomura Y. The interpretation of results of 10-2 visual fields should consider individual variability in the position of the optic disc and temporal raphe. *Br J Ophthalmol*. 2018;102:323–328.
10. Hirooka K, Misaki K, Nitta E, Ukegawa K, Sato S, Tsujikawa A. Comparison of macular integrity assessment (MAIA™), MP-3, and the Humphrey Field Analyzer in the evaluation of the relationship between the structure and function of the Macula. *PLoS One*. 2016;11:e0151000.
11. Balasubramanian S, Uji A, Lei J, Velaga S, Nittala M, Sadda S. Interdevice comparison of retinal sensitivity assessments in a healthy population: the CenterVue MAIA and the Nidek MP-3 microperimeters. *Br J Ophthalmol*. 2018;102:109–113.
12. Matsuura M, Murata H, Fujino Y, Hirasawa K, Yanagisawa M, Asaoka R. Evaluating the usefulness of MP-3 microperimetry in glaucoma patients. *Am J Ophthalmol*. 2018;187:1–9.
13. Igarashi N, Matsuura M, Hashimoto Y, et al. Assessing visual fields in patients with retinitis pigmentosa using a novel

microperimeter with eye tracking: The MP-3. *PLoS One* 2016; 11:e0166666.

14. Asahina Y, Kitano M, Hashimoto Y, et al. The structure-function relationship measured with optical coherence tomography and a microperimeter with auto-tracking: the MP-3, in patients with retinitis pigmentosa. *Sci Rep*. 2017;7: 15766.
15. Amini N, Nowroozizadeh S, Cirineo N, et al. Influence of the disc-fovea angle on limits of RNFL variability and glaucoma discrimination. *Invest Ophthalmol Vis Sci*. 2014;55:7332–7342.
16. Sung MS, Kang YS, Heo H, Park SW. Optic disc rotation as a clue for predicting visual field progression in myopic normal-tension glaucoma. *Ophthalmology*. 2016;123:1484–1493.
17. Bedggood P, Tanabe F, McKendrick AM, Turpin A. Automatic identification of the temporal retinal nerve fiber raphe from macular cube data. *Biomed Optics Express*. 2016;7:4043–4053.
18. Nagai-Kusuhara A, Nakamura M, Kanamori A, Negi A. Association of optic disc configuration and clustered visual field sensitivity in glaucomatous eyes with hemifield visual field defects. *J Glaucoma*. 2009;18:62–68.
19. Sakamoto M, Matsumoto Y, Mori S, et al. Excessive scleral shrinkage, rather than choroidal thickening, is a major contributor to the development of hypotony maculopathy after trabeculectomy. *PLoS One*. 2018;13:e0191862.
20. Jonas RA, Wang YX, Yang H, et al. Optic disc-fovea distance, axial length and parapapillary zones. The Beijing Eye Study 2011. *PLoS One*. 2015;10:e0138701.
21. Huang XR, Zhou Y, Kong W, Knighton RW. Reflectance decreases before thickness changes in the retinal nerve fiber layer in glaucomatous retinas. *Invest Ophthalmol Vis Sci*. 2011;52:6737–6742.
22. Huang XR, Kong W, Qiao J. Response of the retinal nerve fiber layer reflectance and thickness to optic nerve crush. *Invest Ophthalmol Vis Sci*. 2018;59:2094–2103.
23. Fortune B, Burgoyne CF, Cull G, Reynaud J, Wang L. Onset and progression of peripapillary retinal nerve fiber layer (RNFL) retardance changes occur earlier than RNFL thickness changes in experimental glaucoma. *Invest Ophthalmol Vis Sci*. 2013;54:5653–5661.
24. Gardiner SK, Demirel S, Reynaud J, Fortune B. Changes in retinal nerve fiber layer reflectance intensity as a predictor of functional progression in glaucoma. *Invest Ophthalmol Vis Sci*. 2016;57:1221–1227.
25. Inuzuka H, Kawase K, Sawada A, Aoyama Y, Yamamoto T. Macular retinal thickness in glaucoma with superior or inferior visual hemifield defects. *J Glaucoma*. 2013;22:60–64.
26. Badlani V, Shahidi M, Shakoor A, Edward DP, Zelkha R, Wilensky J. Nerve fiber layer thickness in glaucoma patients with asymmetric hemifield visual field loss. *J Glaucoma*. 2006;15:275–280.
27. Yarmohammadi A, Zangwill LM, Diniz-Filho A, et al. Peripapillary and macular vessel density in patients with glaucoma and single-hemifield visual field defect. *Ophthalmology*. 2017; 124:709–719.
28. Sakai T, Sano K, Tsuzuki K, Ueno M, Kawamura Y. Temporal raphe of the retinal nerve fiber layer revealed by modulated fibers. *Jpn J Ophthalmol*. 1987;31:655–658.

Investigative Ophthalmology & Visual Science